Co-operativity between modules within a C3b-binding site of complement receptor type 1

M.D. Kirkitadze[a], D.T.F. Dryden[b], Sharon M. Kelly[c], Nicholas C. Price[c], X. Wang[d], M. Krych[d], J.P. Atkinson[d], P.N. Barlow[a,*]

[a] *The Edinburgh Centre for Protein Technology, Department of Chemistry, University of Edinburgh, West Mains Road, Edinburgh EH9 3JJ, UK*
[b] *Institute of Cell and Molecular Biology, University of Edinburgh, West Mains Road, Edinburgh EH9 3JR, UK*
[c] *Department of Biological Sciences, University of Stirling, Stirling FK9 4LA, UK*
[d] *Department of Internal Medicine, Division of Rheumatology, Washington University School of Medicine, 660 S. Euclid, Box 8045, St. Louis, MO 63110, USA*

Received 11 August 1999

Abstract Complement receptor type 1 (CR1) has 30 modules in its extracellular portion. An understanding of structure-function relationships within CR1 is being assembled gradually from studies of overlapping protein fragments. A CR1 fragment corresponding to modules 16 and 17 was expressed recombinantly as a non-glycosylated protein and its stability and unfolding characteristics studied using biophysical techniques. The results were compared with data collected previously on a CR1 fragment encompassing modules 15, 16 and 17 which together constitute a C3b-binding site (Kirkitadze, M.D., Krych, M., Uhrin, D., Dryden, D.T.F., Smith, B.O., Wang, X., Hauhart, R., Atkinson, J.P. and Barlow, P.N. (1999) Biochemistry 38, 7019–7031). Modules within CR1 were found to co-operate during unfolding. The folding, stability and flexibility of this protein is therefore likely to be a complex function, and not just the sum, of contributions from individual modules.

Key words: CR1; Complement; Module; Protein folding; Differential scanning calorimetry; Fluorescence

1. Introduction

Many proteins of the immune system, the complement and clotting cascades, and the extracellular matrix are mosaic in nature, being built up from protein modules [1]. Each module type is characterised by a consensus sequence, which normally defines a common three-dimensional molecular framework. Functional diversity probably results from at least three factors, namely: the pattern of loops and exposed side chains which are not conserved amongst modules of the same category; the combination within a single protein of various module types; and the intermodular interface or 'junction' which determines the relative orientations of neighbouring modules and hence overall shape and flexibility. Since structures have been determined for many individual module types, attention is now focusing on the intermodular junctions [2,3], and the influence of module-module contacts on the behaviour of the intact protein.

The 220 kDa complement receptor type 1 (CR1) is a representative example of a mosaic protein. Its amino-terminal, extracellular portion consists of 30 modules [4], all belonging to the complement protein (CP) type, also known as 'short consensus repeats' (SCRs), and CR1 is a member of the regulators of complement activation (RCA) family [5]. A recombinant, soluble version of CR1 has therapeutic value [6–8] as an inhibitor of complement and its structure-function relationships are of interest. An understanding of the structure of this large and flexible human glycoprotein is gradually being assembled through studies in solution of overlapping, recombinant fragments [3,9]. A fragment consisting of modules 15–17 (CR1∼15–17) encompasses one of two nearly identical C3b-binding sites in CR1 [10] – the other is found in modules 8–10. The results obtained previously [3] for three CR1 fragments composed respectively of modules 15–17, modules 15, 16 and module 16 (i.e. CR1∼15–17, CR1∼15,16 and CR1∼16) demonstrated that the junction between modules 16 and 17 is the least stable part of Cr1∼15–17 being the first to melt with increasing temperature or denaturant concentration. This event is followed by unfolding of module 17 along with the 15–16 junction, which is more extensive and stable than the 16–17 junction. Finally modules 15 and 16 undergo unfolding at very similar temperatures/concentration of denaturant, apparently adopting an intermediate expanded stage prior to arriving at the random coil state. We now present biophysical data on a fragment of CR1 comprising of modules 16 and 17 (CR1∼16,17, Fig. 1), in order to complement information obtained from the previous study.

2. Materials and methods

2.1. Purification

The cDNA encoding non-glycosylated CR1∼15–17 [3] was used as a template for the polymerase chain reaction amplification of CR1∼16,17 (amino acids 961–1092 of the mature CR1). The 5′ primer for PCR amplification, TCGAGAAAAGAGAGGCTGAAGCTAAATCATGTAAAACTCCTCCAGA and the 3′ primer TTTCTCGAGTTAAATGCACTGAGGGGCGGG, each contain an *Xho*I site. In addition, the 3′ primer contains a translational stop codon. The amplified cDNA was ligated into pPIC9 [11]. Expression of the secreted CR1∼16,17 was performed in the yeast vector *Pichia pastoris* as described [3]. The protein migrated as a single band of about 18 kDa under non-reducing conditions on sodium dodecyl sulphate-polyacrylamide gel electrophoresis. The amino-terminal sequence was

*Corresponding author. Fax: (+44) (131) 650 7155.
E-mail: barlow@chem.ed.ac.uk

Abbreviations: CR1, complement receptor type 1; CR1∼16,17, etc., 16th and 17th modules etc. of CR1; DSC, differential scanning calorimetry; CD, circular dichroism; NMR, nuclear magnetic resonance; HSQC, heteronuclear single quantum coherence; VCP, Vaccinia virus complement control protein; GdmCl, guanidinium chloride; ΔH^{cal}, calorimetric enthalpy

PII: S0014-5793(99)01205-3

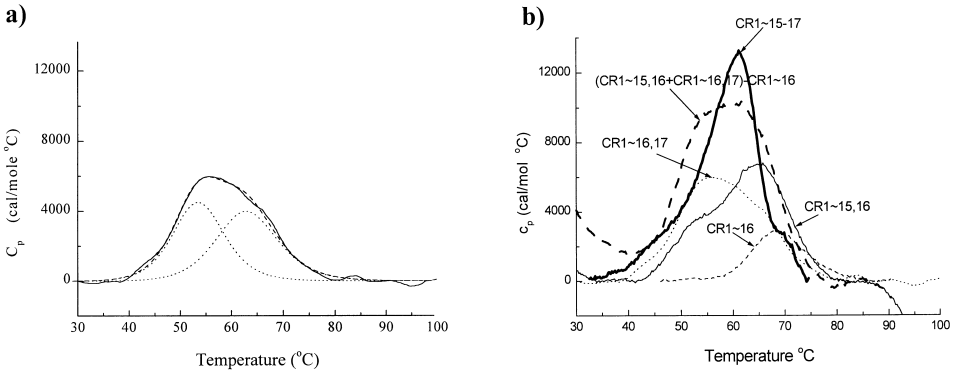

Fig. 1. Differential scanning calorimetry profiles. (a) Profile of CR1∼16,17. Experimental data after base-line subtraction are shown by the solid line. The dashed line indicates the computer-fitted data. (b) Experimental calorimetric profiles for CR1 fragments [3] are shown (short dashes, CR1∼16,17; thick line, CR1∼15–17; thin line, CR1∼15,16; long dashes, CR1∼16; thick dashed line, CR1∼15,16+CR1∼16,17−CR1∼16).

confirmed by amino acid sequencing. As in other constructs, the CR1∼16,17 native sequence was preceded by Glu-Ala-Glu-Ala, derived from the signal peptide of *P. pastoris* α-factor. The yield of the protein was ∼50 mg l^{-1}. The protein was purified according to the procedure used for other CR1 derivatives produced in this system described earlier [3]. Western blots demonstrated that the protein was recognised by two monoclonal anti-CR1 antibodies, 3D9 [12] and J3B11 [13] as well as by a polyclonal anti-CR1 [14]. This suggests that the overall structure of recombinant CR1∼16–17, as produced in *P. pastoris*, has a native structure. Subsequently, the protein fragment was shown to have nuclear magnetic resonance (NMR) and circular dichroism (CD) spectra that are highly characteristic of properly folded CP modules. A buffer of 20 mM sodium phosphate, pH 6.5, was used in all subsequent experiments unless stated otherwise.

2.2. Differential scanning calorimetry (DSC)

Differential scanning calorimetry was conducted as described previously [3]. The partial molar heat capacity and melting curve were analysed using standard procedures [15]. The data were processed using the software ORIGIN 2 (Microcal). The protein concentration was 0.5–2 mg ml^{-1} as determined by measurement of absorbance at 278 nm according to a calculated [16] extinction coefficient of 1.08 for a 1 mg ml^{-1} solution of CR1∼16,17, with a path-length of 1 cm.

2.3. Fluorescence spectroscopy

Measurements of intrinsic tryptophan fluorescence were performed as previously described [3,9]. For the current analysis the change in fluorescence intensity as a function of denaturant was analysed by GRAFIT (Erithacus Software, Staines, UK) with equations [17] for one or two independent two-state unfolding transitions.

2.4. Nuclear magnetic resonance spectroscopy

These measurements were performed with the kind assistance of Drs. Dusan Uhrin and Brian Smith (University of Edinburgh) on spectrometer operating at 600 MHz (proton frequency) as described [3]. ^{1}H-^{15}N Heteronuclear single quantum coherence (HSQC) spectra [18] were acquired on 0.3–0.6 mM samples of recombinant ^{15}N-labelled CR1∼16,17 for 2–8 h each, at a temperature of 25°C, using a composite-pulse WATERGATE for water suppression [19]. Selected, representative cross-peaks within a well-dispersed region of the HSQC spectrum were assigned to module 16 (but not to specific residues) by reference to the published assignments for the backbone ^{15}N and ^{1}H chemical shifts of CR1∼15,16 [3]. Other cross-peaks within this region, that are absent from the spectra of CR1∼15,16 and of CR1∼16 were assigned to module 17.

2.5. Circular dichroism measurements

Circular dichroism experiments were performed as described previously [3]. The protein concentration was 0.2 mg ml^{-1}. All measurements were recorded at 25°C. To obtain a plot of percentage total change versus concentration of GdmCl ([GdmCl]), the maximum ellipticity and readings at ±1.0 nm and ±2.0 nm were averaged to smooth the experimental curve.

3. Results and discussion

The aim of this study was to further characterise one of the two nearly identical C3b-binding sites of CR1, the region encompassing modules 15–17. In a previous study, CR1∼15–17 in solution had been subjected to a range of biophysical techniques and the results interpreted with the help of the data collected on sub-fragments, CR1∼15,16 and CR1∼16 [3]. The successful expression of Cr1∼16,17 described in this study has created the opportunity to undertake further analysis of this region. A related study of Cr1∼16,17 based on fluorescence and ultracentrifugation is described elsewhere [9].

3.1. Calorimetric studies

The thermal unfolding of Cr∼16,17 was studied using DSC. The CR1∼16,17 melting profile is complex but may reasonably be fitted to two overlapping transitions (Fig. 1). The total enthalpy value for CR1∼16,17 is 502 kJ mol^{-1} which is close to the total value of 555 kJ mol^{-1} obtained for CR1∼15,16 [5] and approximately double the calorimetric enthalpy of module 16 alone (252 kJ mol^{-1}). This value is higher than those obtained for the pair of CP modules that make up the $GABA_b$ receptor 1a amino-terminus (376 kJ mol^{-1}) [20], and the central pair of CP modules from the Vaccinia virus complement control protein (VCP, 360 kJ mol^{-1}) [21] but it is within the range of enthalpy values obtained for other proteins of approximately this molecular weight [22].

It was shown in the previous study that the first of the three transitions in the calorimetric profile of CR1∼15–17 belongs to melting of the 16–17 junction while the second transition corresponds to melting of both module 17 (melting temperature, $T_m = 57.5$°C) and the 15–16 junction. The third and largest transition (61.5°C) in the profile of CR1∼15–17 corresponds to melting of modules 15 and 16. Thus the second transition (64°C) in the CR1∼16,17 profile is highly unlikely to correspond to module 17 and almost certainly corresponds to the melting of module 16. The first transition (54°C), on the other hand, is likely to be, at least in part, a consequence of melting of module 17. There does not appear to be a separate transition in the profile of CR1∼16,17 corresponding to the melting of the 16–17 junction, unlike the case of CR1∼15–17 where a putative 16–17 junction transition ($T_m = 50.5$°C) was

separated by 7°C from the transition due to module 17 unfolding. In CR1∼16,17, the enthalpy for this process is probably subsumed within the 54°C transition.

3.2. NMR and fluorescence spectroscopy in presence of GdmCl

The NMR technique ^{1}H-^{15}N HSQC spectroscopy was used in conjunction with existing fluorescence spectroscopy data, to probe the stability of CR1∼16,17 modules in the presence of GdmCl and to test hypotheses advanced in earlier work [3,9]. The structural integrity of CR1∼16,17 at [GdmCl] = 0, 1, 2 and 3 was examined. In native buffer (i.e. 0 M GdmCl) CR1∼16,17 yielded a HSQC spectrum (Fig. 2) consistent with a small, folded, monodisperse protein. As expected, many of the approximately 120 cross-peaks may be superimposed with cross-peaks observed previously in the HSQC spectra of CR1∼16, CR1∼15,16 and CR1∼15–17. It was therefore possible to assign cross-peaks in uncrowded regions of the spectrum to amide protons and ^{15}N's within either module 16 or module 17. After addition of GdmCl to a concentration of 1 M, all cross-peaks were weaker. Most are still recognisable but others moved or became undetectable (Fig. 2). There was no detectable peak at the random coil position of Trp which in previous studies had been regarded as symptomatic of the presence of unfolded modules. When the concentration of denaturant was raised to 2 M GdmCl, there was little further change in the spectrum. At 3 M GdmCl (Fig. 2) the HSQC spectrum reveals a substantial loss of tertiary structure. A strong random coil Trp peak (Fig. 2, indicated by arrow) is indicative of unfolded module(s). There were no recognisable dispersed cross-peaks from module 17, however a number of dispersed cross-peaks from module 16 were still present including a cross-peak due to the ring NH of Trp-1013 ($^{1}H_{\delta} = 10.44$ ppm, $^{15}N_{\delta} = 127$ ppm).

For the purposes of this study, intrinsic tryptophan fluorescence data reported previously were analysed, fitted and replotted (Fig. 3). Changes in the HSQC spectra were subsequently used to interpret the fluorescence data. There is a transition in the fluorescence curve of CR1∼16,17 which is nearly complete by 1 M GdmCl. This corresponds to the significant number and extent of changes in the chemical shifts of several backbone ^{15}N and ^{1}H nuclei evident in the HSQC spectra (Fig. 2). Since there was no detectable random coil Trp peak in the HSQC spectrum at 1 M GdmCl, and there is plenty of chemical shift dispersion still present in the spectrum, the modules appear to be folded at 1 M GdmCl. Hence these data are consistent with the notion that it is the 16–17 intermodular junction that unfolds under very mild denaturing conditions and yields a small transition (15% of total change) in the fluorescence plot. Between 1 M GdmCl and 2 M GdmCl there was only a very gradual rise in fluorescence intensity (5% of total change) consistent with the lack of drastic changes in the relevant HSQC spectra. Between 2 M GdmCl and 3 M GdmCl there was a steeper change (accounting for 20% of the total) consistent with the major changes in the HSQC spectrum. Thus these data are consistent with the

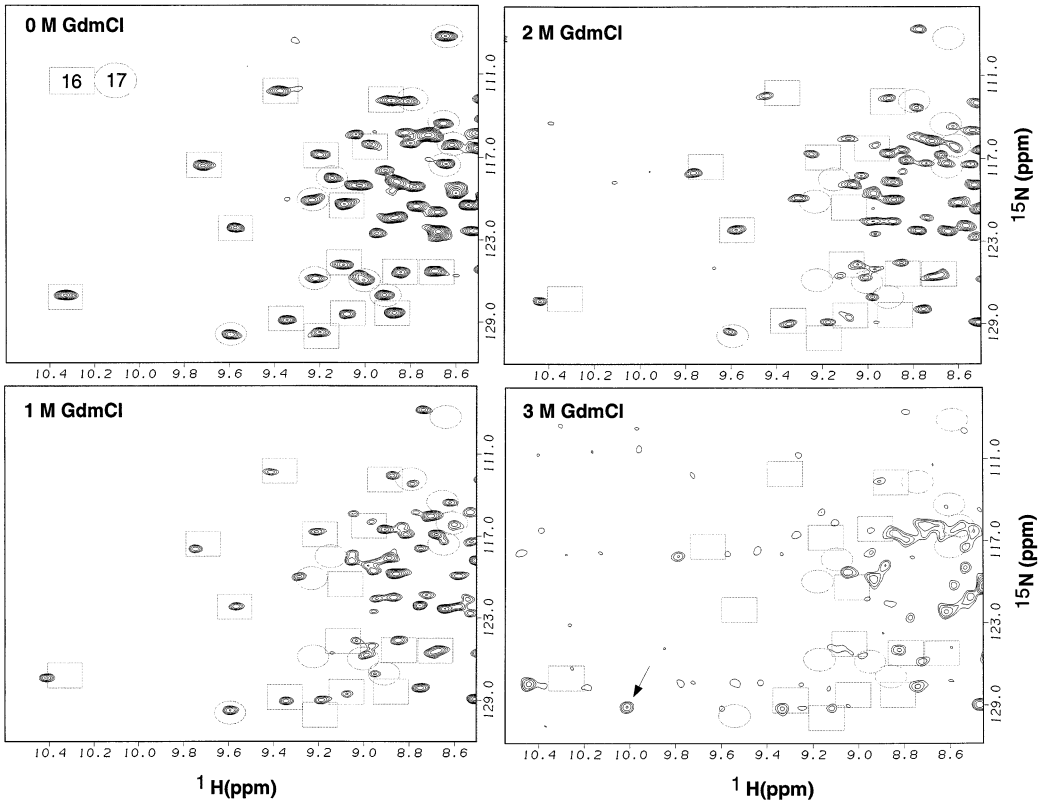

Fig. 2. A series of $^{1}H^{15}N$ HSQC spectra collected on CR1∼16,17. Spectra were recorded at 25°C. Shown is a region containing well-dispersed cross-peaks. Per module assignment of selected cross-peaks at 0 M GdmCl (top left) was achieved as described in the text. Cross-peaks assigned to module 16 are enclosed in rectangles, cross-peaks assigned to module 17 are enclosed in ovals. The positions of the cross-peaks detected at 0 M GdmCl are also indicated by rectangles or ovals in the spectra collected in the presence of increasing [GdmCl] as indicated. The arrow indicates cross-peak due to Trp ring NH in random coil.

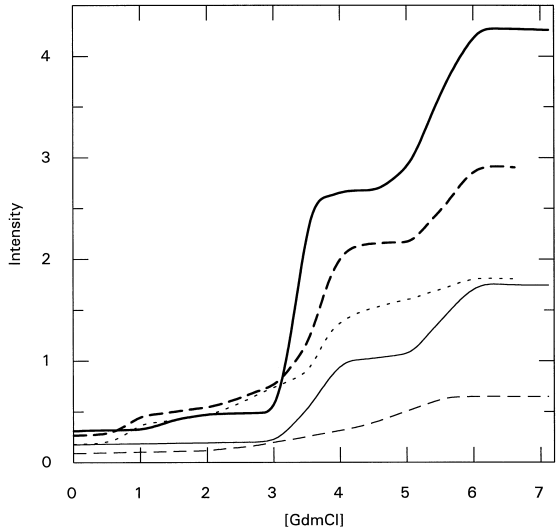

Fig. 3. Intrinsic tryptophan fluorescence as a function of [GdmCl]. Shown are the fitted (see text) curves for CR1∼16,17 (based on data collected previously [9]) along with the fitted curves for the other CR1 fragments studied [3]. Also shown is the outcome of adding together the curves for CR1∼16,17 and CR1∼15,16 and subtracting the curve for CR1∼16. The same symbols are used as in Fig. 1.

onset of module unfolding, with module 17 being unfolded to a greater extent than module 16 at 3 M GdmCl.

3.3. Studies using CD

The GdmCl-induced unfolding of CR1∼16,17 was also monitored by CD (Fig. 4) to complement the NMR, DSC and fluorescence studies. Like other fragments derived from the RCA family and related proteins – for example CR1∼15–17 [3], CR1∼1–3 [23], the central two modules of both VCP and decay accelerating factor, and the amino-terminal portion of metabotropic $GABA_b$ receptor 1a [20] – CR∼16,17 show positive ellipticity in the far-UV region. This has previously been interpreted as reflecting the environment of Trp located on β-strands [24]. Fig. 4 shows the far-UV CD spectra of CR1∼16,17 obtained over a range of [GdmCl]. There was a substantial (40%, Fig. 4, inset) loss of characteristic positive CD signal (230–240 nm) in the range 0–2 M GdmCl. This was followed by a more gradual loss of signal and a 6 M GdmCl, the positive 230–240 nm peak had disappeared indicating that the conformation was random coil. Only about 20–25% of total increase in Trp fluorescence was observed in the range 0–2 M GdmCl, while NMR indicated that both modules were substantially intact at 2 M GdmCl. Thus the loss of CD signal must be due primarily to loss of the intermodular junction. That ellipticity is so sensitive to junction melting could be explained by the proximity of the Trp of module 17 to the junction with module 16. In the cases of CR1∼15–17 and CR1∼15,16, only a minor loss of ellipticity was observed below 2.5 M GdmCl (about 8%). These differences in ellipticity as a function of [GdmCl] between the two module pairs could be explained by the more stable nature of the 15–16 junction, and by the fact that each tryptophan does not make an equal contribution to the total ellipticity.

3.4. Implications for the structure of a C3b-binding site of CR1

Having described our interpretation of our results on CR1∼16,17 and having placed them in the framework of our studies of CR1∼15–17, we now discuss their wider implications for the structure and flexibility of CR1.

If all three CP modules were separated by flexible linkers such that three-dimensional structures were not strongly influenced by neighbouring modules, then structure-dependent properties of individual modules such as ellipticity and calorimetric enthalpy would be additive, i.e. the whole would be a sum of its parts. Moreover, if modules unfold in ways that are independent of each other, then calorimetric profiles and plots of intrinsic tryptophan fluorescence versus [GdmCl] would also be additive. On the other hand, T_m's, and [GdmCl] required to achieve mid-point of unfolding transition ($[GdmCl]^{mid}$) of specific modules should, in these hypothetical circumstances, be independent of context. Thus the key issue of the extent of interactions between CP modules may be gauged from a comparison of theoretical values derived from individual contributions, with experimental data.

The results of such an analysis are presented in Fig. 5, and in Figs. 1 and 3. Melting temperatures (Fig. 5) clearly are dependent on context. Module 16, for example, is more stable to temperature as a single module than when part of a larger fragment, as discussed in Kirkitadze et al. [3]. It now emerges that it is significantly more stable when attached to module 15 than when attached to module 17. It was also noted previously that the attachment of module 17 to CR1∼15,16 appears to destabilise module 15 by 4°C; it now appears that addition of module 15 to CR1∼16,17 results in stabilisation of module 17 by 5°C. The interesting consequence is that within the triple module fragment there is a convergence of melting points so that the difference in melting temperature between modules 15 and 16 is only 4°C compared to 16.5°C (i.e. T_m of CR1∼16 cf. T_m of module 15 in CR1∼15,16). Comparisons of $[GdmCl]^{mid}$ values at the module level are more difficult due to the inferred existence of partially folded intermediates [3]. However it appears (Fig. 4) that the 16–17 junction is more stable within the triple module fragment than it is in the absence of module 15.

Although the three single modules are not available, the data collected for CR1∼16,17 allow the principal of additivity to be tested. Fig. 5 shows the outcome of summing the

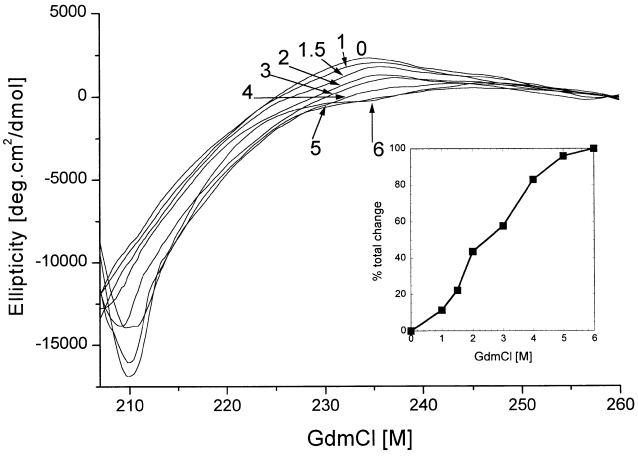

Fig. 4. Guanidinium-induced unfolding followed by circular dichroism. A series of far-UV CD spectra for CR1∼16,17 were collected over a range of [GdmCl], as indicated by the numerals and arrows on the figure. Inset: Plot of % total change in ellipticity versus [GdmCl].

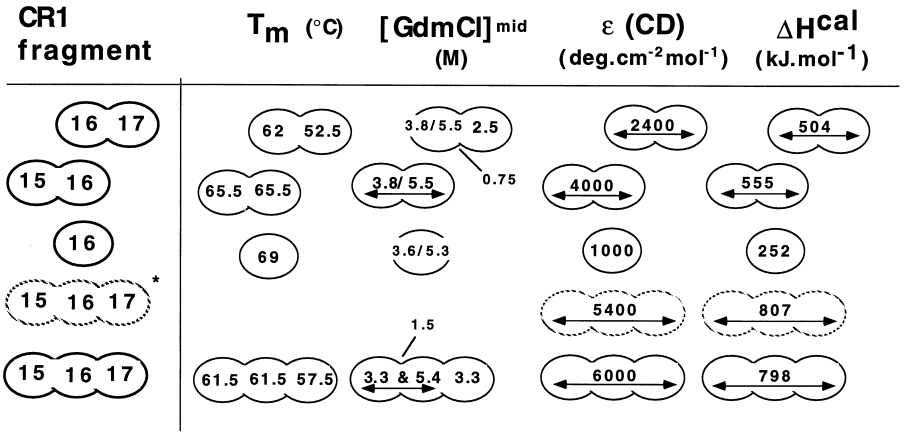

Fig. 5. Summary of results obtained for the various CR1 fragments studied. Modules are indicated by oval symbols and schematic representations of fragments are drawn with the amino-terminus to the left; where available, values relating to individual modules are written inside that module's symbol. Where the numbers given are for more than one module, this is indicated by double-headed arrow indicating the modules involved. Where a value of [GdmCl] for an intermodular junction is available, this is indicated.

maximum ellipticity values of CR1∼15,16 and CR1∼16,17, then subtracting the maximum ellipticity value of module 16. The hypothetical value obtained is within experimental error of the measured value for CR1∼15–17. A similar treatment of calorimetric enthalpies (Fig. 5) also yields numbers within error of measured ones. These results are consistent with the fact that changes in NMR chemical shifts for module 16 in different contexts are limited [3], and supports the theory that the structures of modules and of intermodular junctions are broadly independent of context. The experimentally determined structure pairs of three CP modules are now available (two by NMR [25,26] and one by crystallography [27]). All show that CP modules are joined end-to-end via small interfaces to form highly extended structures with a range of intermodular orientations and apparent degrees of flexibility. Hydrodynamic data for CR1∼16,17 indicate that it is also elongated with an axial ratio of ∼5:1 while CR1∼15–17 has an axial ratio of ∼6:1. Thus it is unsurprising that structures of modules, which are compact and globular, are not influenced strongly by neighbouring modules.

That melting temperatures of modules and stabilities of junction are influenced by neighbouring modules while global structures are not, may be a consequence of the different unfolding pathways that are available to modules within different contexts. Unfolding of module 16 in isolation involves many intermediates and is a gradual function of temperature or [GdmCl] compared with unfolding of module 16 when it is part of a larger fragment. Fig. 5, right part shows the outcome of summing calorimetric profiles for CR1∼15,16 and CR1∼16,17 and subtracting the profile of CR1∼16. The hypothetical profile is very much broader and significantly lower than the experimental one. This emphasises the degree of co-operativity that exists between modules in the melting of the multimodular fragment. A similar exercise was undertaken for the fluorescence intensity versus [GdmCl] curves (Fig. 3). Although the shape of the theoretical curve resembles the experimental one at [GdmCl] > 4 M, agreement in the range (1–4 M GdmCl) where junctions unfold and modules are partially disrupted is poor.

It is of interest (Fig. 3) that while denaturant-induced unfolding of module 16 in the context of CR1∼15,16 or CR1∼15–17, is associated with a sharp transition when part of CR1∼16,17, module 16's unfolding transition is more gradual. That module 15 has a bigger influence than module 17 on the unfolding of module 16 reinforces a previous suggestion, that the 15–16 interface is more extensive and stable than the 16–17 one.

Taken together, these studies show that multimodular proteins may have overall properties of stability and flexibility that are not just a sum of the individual contributions from their component modules. In the case of CR1, segmental flexibility within key regions may be essential for function since there are three ligand-binding sites (CR1∼15–17, CR1∼8–10 and CR1∼15–17) each spread out over several neighbouring modules. That intermodular contacts play an important role in the biological function of CR1 is borne out by the deleterious effects on activity of mutations [28] of interfacial residues. The co-operativity observed between some CP modules during unfolding may also have implications for folding of the CR1 chain which, a priori, appears to be a complex process since there are 1800 amino acids and 60 disulphides in its N-terminal portion. The data presented here also indicate that it may be misleading to consider individual CP modules as evolutionary building blocks that can be readily interchanged via a process of exon shuffling. Finally these data have implications for the widespread use of domain swaps for functional studies, and protein engineering for the production of versions of soluble CR1 with improved therapeutic applications.

Acknowledgements: M.D.K. is funded by the Human Frontiers Science program. D.T.F.D. is funded by Royal Society of Great Britain. This work was also funded by the Edinburgh Centre for Protein Technology. The Circular Dichroism facility in Stirling University is funded by BBSRC. Work in St. Louis was supported in part by funding from the National Institute of Health (R01 AI41592) and from CytoMed Inc. (Cambridge, MA). J.P.A. and Washington University have a financial interest in CytoMed Inc.

References

[1] Doolittle, R.F. (1985) Trends Biochem. Sci. 114, 233–237.
[2] Spitzfaden, C., Grant, R.P., Mardon, H. and Campbell, I.D. (1997) J. Mol. Biol. 265, 565–579.
[3] Kirkitadze, M.D., Krych, M., Uhrin, D., Dryden, D.T.F., Smith, B.O., Wang, X., Hauhart, R., Atkinson, J.P. and Barlow, P.N. (1999) Biochemistry 38, 7019–7031.
[4] Klickstein, L.B., Bartow, T.J., Miletic, V., Robson, L.D., Smith, J.A. and Fearon, D.T. (1988) J. Exp. Med. 168, 1699–1717.
[5] Reid, K.B.M., Bentley, D.R., Campbell, R.D., Chung, L.P., Sim, R.B., Kristensen, T. and Tack, B.F. (1986) Immunol. Today 7, 230–234.
[6] Weisman, H.F., Bartow, T., Leppo, M.K., Marsh, H.C., Carson, G.R., Concino, M.F., Boyle, M.P., Roux, K.H., Weisfeldt, M.L. and Fearon, D.T. (1990) Science 249, 146–151.
[7] Hebell, T., Ahearn, J.M. and Fearon, D.T. (1991) Science 254, 102–105.
[8] Kalli, K.R., Hsu, P. and Fearon, D.T. (1994) Springer Semin. Immunopathol. 15, 417–431.
[9] Kirkitadze, M.D., Jumel, K., Harding, S.E., Dryden, D.T.F., Krych, M., Atkinson, J.P. and Barlow, P.N. Progress in Colloid and Polymer Science, in press.
[10] Krych, M., Hauhart, R. and Atkinson, J.P. (1998) J. Biol. Chem. 273, 8623–8629.
[11] Scorer, C.A., Clare, J.J., McCombie, W.R., Romanos, M.A. and Sreekrishna, K. (1994) Bio/technology 12, 181–184.
[12] O'Shea, J.J., Brown, E.J., Seligmann, B.E., Metcalf, J.A., Frank, M.M. and Gallin, J.I. (1985) J. Immunol. 134, 2580–2587.
[13] Cook, J., Fischer, E. and Boucheiz, C. (1985) Mol. Immunol. 22, 531–539.
[14] Makrides, S.C., Scesney, S.M., Ford, P.J., Evans, K.S., Carson, G.R. and Marsh Jr., H.C. (1992) J. Biol. Chem. 267, 24754–24761.
[15] Privalov, P.L. and Potekhin, S.A. (1986) Methods Enzymol. 131, 40–51.
[16] Sober, H.A. (1970) in: Handbook of Biochemistry, 2nd Edn., CRC Press Inc., Boca Raton, FL, pp. B75–76.
[17] Hamaguchi, K. (1992) in: The Protein Molecule: Conformation Stability and Folding, Springer Verlag, Berlin.
[18] Bodenhausen, G. and Ruben, D.J. (1980) Chem. Phys. Lett. 69, 185–189.
[19] Mori, S., Abeygunawardana, C., Johnson, M.O. and van Zijl, P.C.M. (1995) J. Magn. Reson. B 108, 94–98.
[20] Hawrot, E., Xiao, Y., Shi, Q.-L., Norman, D., Kirkitadze, M. and Barlow, P.N. (1998) FEBS Lett. 432, 103–108.
[21] Kirkitadze, M.D., Henderson, C., Price, N.C., Kelly, S.M., Mullin, N.P., Parkinson, J., Dryden, D.T.F. and Barlow, P.N. Biochem. J., submitted.
[22] Privalov, P.L. (1979) Adv. Protein Chem. 33, 167–241.
[23] Clark, N.S., Dodd, I., Mossakowska, D.E., Smith, R.A.G. and Gore, M.G. (1996) Protein Eng. 9, 877–884.
[24] Freskgård, P.O., Mårtensson, L.G., Johansson, P., Jonsson, B.H. and Carlsson, U. (1994) Biochemistry 33, 14281–14288.
[25] Reid, K.B.M., Bentley, D.R., Campbell, R.D., Chung, L.P., Sim, R.B., Kristensen, T. and Tack, B.F. (1986) Immunol. Today 7, 230–234.
[26] Wiles, A.P., Shaw, G., Bright, J., Perczel, A., Campbell, I.D. and Barlow, P.N. (1997) J. Mol. Biol. 272, 253–265.
[27] Casanovas, J.M., Larvie, M. and Stehle, T. (1999) EMBO J. 18, 2911–2922.
[28] Krych, M., Clemenza, L., Howdeshell, D., Hauhart, R., Horcade, D. and Atkinson, J.P. (1994) J. Biol. Chem. 18, 13273–13278.